



Comparative Analysis of Solar Photovoltaic System MPPT Techniques

Ramya Gullapelly¹, Jyothsna Nakka², A.Thirumala³, Sreelatha Jakkula⁴, P.Shankar Babu⁵
1, 2, 3, 4 Assistant Professor, Department of Electrical and Electronics Engineering, Vaagdevi College of Engineering, Warangal, Telangana-506005, India.

5 Associate Professor, Department of Electrical and Electronics Engineering, Vaagdevi College of Engineering, Warangal, Telangana-506005, India.

Abstract

Solar photo voltaic (PV) has established itself as the most stable method of solar energy collecting. Temperature and sun radiation are two factors that affect a solar PV system's production throughout the day. The maximum power point (MPP) on the solar PV output characteristics curve varies as a result of this. Thus, in order to track the MPP and maximize the power output from the PV systems, different Maximum Power Point Tracking (MPPT) strategies are employed. This research presents a detailed simulation-based analysis that compares three commonly used MPPT algorithms: Particle Swarm Optimization (PSO), Cuckoo Search (CS), and Perturb and Observe (P&O) using MATLAB Simulink. These MPPT algorithms are used to control a DC-DC Boost converter's duty cycle. The three algorithms are evaluated based on how well they track in terms of tracking efficiency, accuracy, and speed. Under partial shade and rapidly changing irradiance conditions, the CS MPPT algorithm demonstrated the best tracking efficiency of the three.

Keywords- Maximum Power Point Tracking, Photovoltaic, Particle Swarm Optimization, Cuckoo Search, Perturb and Observe

I. INTRODUCTION

In recent times, producing electricity with solar photovoltaic (PV) technology has emerged as the most practical choice. The usage of solar photovoltaic systems (PV) for power generation has increased recently due to the depletion of fossil fuel supplies and growing worries about the environmental effects of fossil fuel use. Power produced by photovoltaic cells is a low-maintenance, clean energy source that produces little noise.

Solar irradiation, temperature, and shading conditions are some of the elements that affect the amount of energy produced by PV modules [1]. The voltage-current (V-I) characteristics of PV modules are non-linear. PV modules have a single point on their voltage-power (V-P) characteristic curve where they produce their maximum power (P_{max}). Variations in the surrounding conditions also affect MMP. This results in a mismatch between the characteristics of the load and the source, lowering the maximum power supplied to the load. In order to minimize power loss and match the characteristics of the PV module with the load, maximum power point tracking, or MPPT, is utilized[1,2].The MPPT controller facilitates the regulation of a DC-DC converter's duty cycle, serving as a mediator between the PV modules and the load.

Many MPPT approaches are available in the literature that can be used in various PV applications to extract the maximum power supplied by the PV modules. Perturb and Observe (P&O), Fractional Short Circuit Current (FSCC), Incremental Conductance (IC), etc. are a few frequently utilized MPPT techniques. Particle

Swarm Optimization (PSO), fuzzy logic, and artificial neural networks (ANN) are a few sophisticated soft computing-based MPPT methodologies.

The many MPPT approaches vary from one another in a variety of ways, including speed of convergence, ease of hardware implementation, complexity, effectiveness, and the number of sensors needed [3].

P&O is the most used MPPT method because of its simplicity, dependability, and ease of application. However, this approach has two significant drawbacks: First, there are constant oscillations in output power as one approaches the MPP, which lowers the energy yield. Second, energy loss results from the operating point shifting away from the MPP locus due to this method's inability to adapt to the rapidly changing irradiance [4]. Certain MPPT techniques based on soft computing are gaining popularity as solutions to these issues. Two efficient and straightforward meta-heuristic techniques for tracking MPP are Particle Swarm Optimization (PSO) and Cuckoo Search (CS). Under partial shading conditions (PSC), these MPPT algorithms can extract the global maximum power point (GMPP). The identification of the shade pattern for the GMPP location is not necessary for these procedures [5]. In order to compare the outcomes with the traditional incremental resistance-based MPP tracker method, Rezk et al. [5] investigated PSO and CS. Using MATLAB, the three MPP tracking strategies were compared for partial shading. Comparing PSO and CS to incremental resistance, MPP convergence was more rapid. Because CS-based trackers required less tracking time than PSO, they were superior. Mosaad et al. [6] used CS and contrasted the MPPT technique's outcomes with ANN- and IC-based MPPT approaches. In comparison to IC and ANN under various settings, it was discovered that CS provided the most power. Additionally, there were no variations in output power while approaching MPP. A comparison of PSO and traditional MPPT approaches (IC, P&O) for PV systems was done by Koad and Zobaa [7]. Cuk converter is used in MATLAB to implement these MPPT algorithms and compare them based on tracking speed, accuracy, cost, and performance. Simulations shown that PSO can reliably track MPP in every scenario. When compared to other approaches, it also has a high tracking efficiency. In addition, it is simpler to construct and has faster convergence than IC and P&O. CS simulations were run by Ahmed and Salam [8] in order to track MPP in PV systems. The outcomes were compared to the traditional P&O approach. The results of the simulation demonstrated that even in the face of rapidly varying meteorological conditions, the CS approach monitors the MPP with zero steady state oscillations.

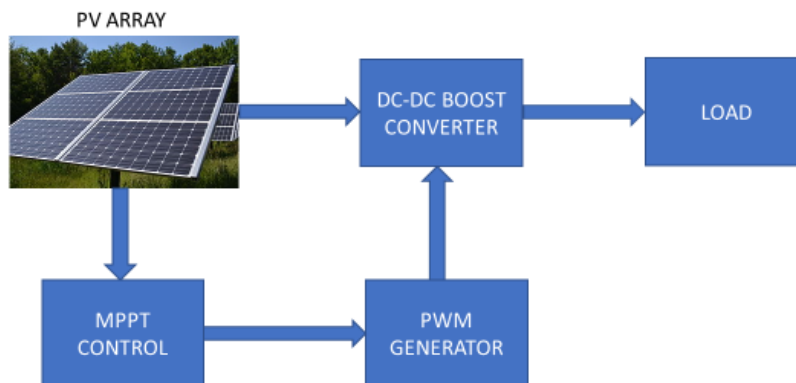


Fig.1. PV System with MPPT

In the present work, a correlative study of three MPPT techniques viz, PSO, CS and P&O is done at standard test condition (STC) as well as at the changing conditions of irradiance. The article is organized in five sections. Section I encloses the introduction and objective. Section II contains the description of the system and its component. Section III discusses the MPPT techniques used. Interpretation of the simulation results is discussed in Section IV. Conclusion is of the study is stated in Section V.

II. SYSTEM COMPONENTS

Fig. 1 shows the schematic of a PV system with maximum power point tracking. A DC-DC converter should be used to match the impedance between the PV array and the load during changing climatic conditions in order to track MPP. The MPPT controller obtains the real-time operational parameters needed by the controlling MPPT algorithm to control the duty cycle of the DC-DC converter [9]. The ensuing subsections address the modelling of the elements in the schematic shown above.

A. PV modeling

Fig. 2 shows the equivalent electrical circuit of a PV cell with a single diode. Its photocurrent (I_{ph}) is produced by a light-dependent current source. A diode is connected in parallel to the source of current, signifying the diffusion current phenomenon (I_d). Series resistance (R_s) is a representation of the contact resistance between the silicon and the metal contact. Shunt resistance is a measure of power loss resulting from manufacturing flaws (R_{sh}).

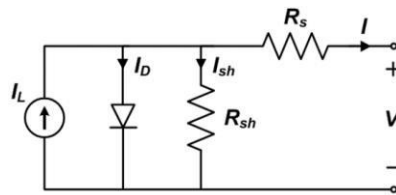


Fig.2. Equivalent electrical circuit of the single diode solar cell model

The output current of solar cell is directly proportional to the solar irradiation falling on it. The series combination of solar cells forms a PV module whose current is given by(1):

$$I = N_p I_{ph} - N_p I_s \left[\exp \left(\frac{v_{pv} + \left(\frac{N_s}{N_p} \right) R_s I}{n_s a v t} \right) - 1 \right] - \left[\frac{v_{pv} + \left(\frac{N_s}{N_p} \right) R_s I}{\left(\frac{N_s}{N_p} \right) R_p} \right] \quad (1)$$

Where the output current (A) of PV module is designated by I , V_{pv} is output voltage (V) of the PV array, N_s and N_p represent the number of PV modules connected in series and parallel respectively, n_s is the number of PV cells connected in series in a single string, R_s and R_p represents series and parallel resistances (Ω) of PV module respectively, a represents p-n junction ideality factor. The PV module modeled in this paper is Solar ex MSX-60 whose specifications are compiled in Table 1.

TABLE I. SPECIFICATIONS OF SOLAREX MSX-60

Parameters	Abbreviation	Values
No. of series connected cells	N_s	36
Maximum power	P_{mp}	59.85W
Maximum current	I_{mp}	3.5A
Maximum voltage	V_{mp}	17.1V

Short circuit current	I_{sc}	3.8A
Open circuit voltage	V_{oc}	21.1V
Temperature coefficient of V_{oc}	α	-0.8%/°C
Temperature coefficient of I_{sc}	β	0.00247%/°C

In this investigation, a series combination of four of these PV modules was used. Fig. 3 shows the I-V and P-V curves of a PV array made up of four series-connected modules at various temperatures (T) and levels of solar irradiation (G).

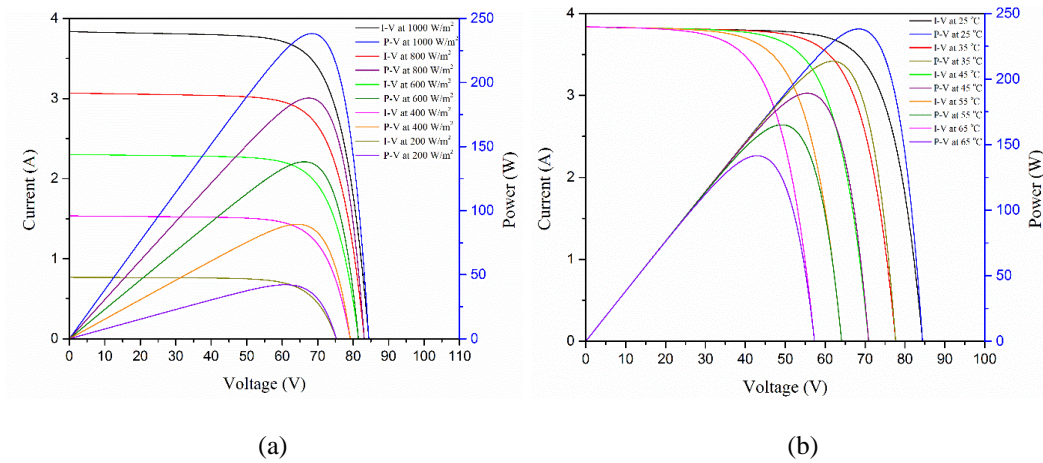


Fig. 3. (a) I-V and P-V characteristics curves at varying G and T=25 oC (b) I-V and P-V characteristics curves at varying T and G=1000W/m²

B. DC-DC Boost Converter

To transfer the maximum power from a PV module to a load, a boost converter is used in this instance (Fig. 4.).The voltage is increased from the supply side to the load side with the aid of the boost converter. When switch (S) is closed, the boost converter is activated. The inductor current increases when the converter is in the ON state. Conversely, when switch (S) is opened, the boost converter enters an OFF state. Here, the load (R), capacitor (C), and diode (D) are all receiving current.

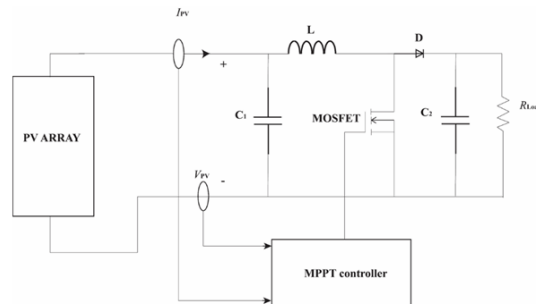


Fig. 4. Boost converter circuit with PV source and resistive load

TABLE II. VARIOUS PARAMETERS OF DC-DC CONVERTER

Parameters	Abbreviation	Value
Resistor	R	50Ω
Inductor	L	1.15mH
Capacitor	C1	10μF
Capacitor	C2	470μF

The input and output voltages of the boost converter, V_{in} and V_{out} , respectively, are connected to one another by the following relation:

$$\frac{V_o}{V_i} = \frac{1}{1-d} \quad (2)$$

where d represents duty cycle of the boost converter. The output voltage always exceeds the input voltage as described by (2) as the duty cycle ranges from 0 to 1. The parameters of DC-DC boost converter are summarised in Table 2.

III. MPPT ALGORITHMS

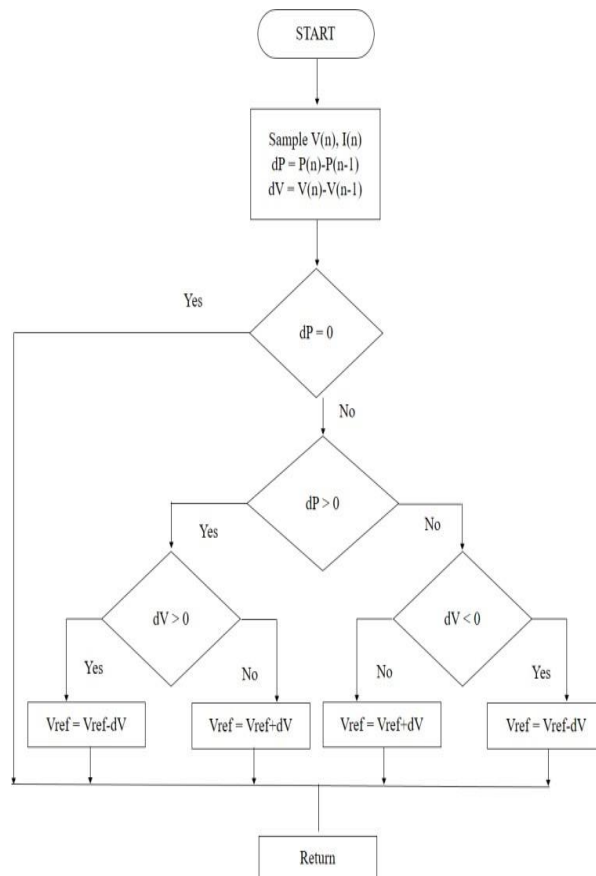
1) Perturb and Observe (P&O)

The PV array's terminal voltage or current is periodically perturbed (increasing or decreasing), and the PV output power is compared to the output power of the preceding perturbation cycle. The control algorithm shifts the operating point in the desired direction if the module's operating voltage changes and its power increases; otherwise, it moves in the other direction. In the subsequent cycle of perturbation, the P&O algorithm operates on a similar concept [10].

Fig. 5 displays the flow diagram for the P&O MPPT approach. This approach has been employed before in [11]. a tiny change in power (P) brought about by a slight increase in system voltage (V). The operational voltage of the system perturbs in the same direction as the increase when the power is changed positively. Conversely, in the event that P is negative, the operating voltage will travel in the opposite direction of the increase. This approach results in oscillations in the output power even after achieving the maximum power point, which in turn causes power losses. This is because the terminal voltage of the PV array is disturbed throughout each MPPT cycle. It is a significant drawback of this approach. Additionally, under conditions when solar irradiation varies often, this method occasionally fails to discover MPP.

2) Particle Swarm Optimization (PSO)

It is based on how flocks of birds behave. It takes into account an n-dimensional swarm of particles, each of which represents a solution. Based on their own prior experiences as well as those of their neighbors, the particles in the multidimensional space continuously modify their position to locate the desired place. Every particle's position is affected by the best particle in the vicinity ($P_{best\ i}$). The optimal solution discovered by the entire particle population (G_{best}) also affects each particle's position [12]. Depending on the current value, the initial velocity is increased or decreased to move the particle into the optimal place. If the current value of position is less than best value then there is an increase in the velocity value and vice versa. The position (x_i) of the particle is adjusted based on [13]:



$$x_i^{k+1} = x_i^k + v_i^{k+1} \quad (3)$$

Fig. 5. Flow diagram showing operation of Perturb and Observe method

The velocity (v_i) in (3) is calculated using [13]:

$$v_i^{k+1} = wv_i^k + c_1r_1\{P_{best\ i} - x_i^k\} + c_2r_2\{G_{best} - x_i^k\} \quad (4)$$

Where I is the inertia weight and C_1 and C_2 are the coefficients of acceleration. The best personal position of particle i is represented by $P_{best} i$, whereas the neighbourhood position of particle i , $r_1, r_2 \in U$ is represented by G_{best} . Fig. 6 displays the PSO flow diagram. There has already been discussion of this approach in [13].

3) Cuckoo Search (CS)

It is predicated on the brood parasitism technique, which Cuckoo birds use to lay their eggs (laying eggs in the nests of other birds). CS is governed by three fundamental rules [14]: (a) One egg will be laid by each cuckoo at a time, and it will be placed in whatever nest is chosen at random. (b) The best nest that produces the best eggs will be handed down to the next generation.

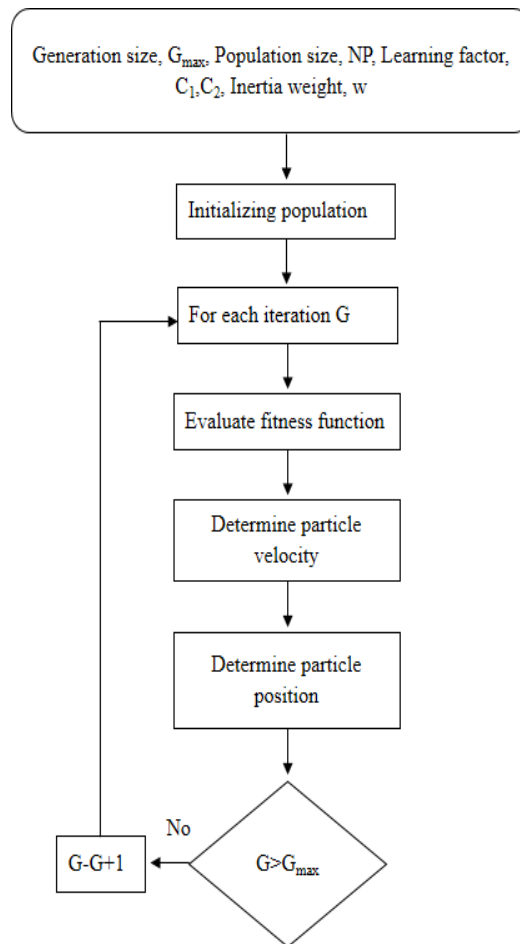


Fig. 6. Flow diagram of Particle Swarm Optimization method

(c) The number of convenient nests is predetermined, and P_a is the likelihood that the host bird will find the egg deposited by a cuckoo in one of these predetermined nests, where $P_a \in [0, 1]$. In this instance, the cuckoo birds stand in for the particles tasked with solving the problem, and the cuckoo bird eggs stand in for the current iteration's solution.

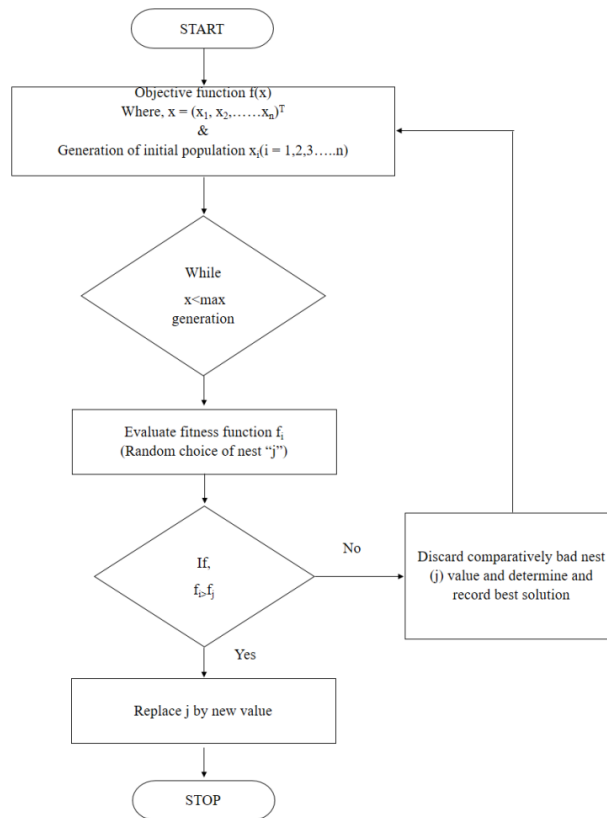


Fig. 7. Flow diagram showing Cuckoo Search method

The CS algorithm follows the Lévy distribution, which allows it to obtain local maxima points and, at the same time, shortens the tracking time required to reach global maximum power point [15]. The flow diagram of CS [16] is presented in Fig. 7.

IV. RESULTS AND DISCUSSION

The three MPPT (P&O, PSO, and CS) approaches have been compared in the following three scenarios: Standard test circumstances, partial shade, and rapidly fluctuating solar radiation are the first three. Fig. 8 displays the MATLAB Simulink model for the system that was designed. Based on their tracking speed and tracking efficiency (Teff), which is computed using [17]: The MPPT algorithms are compared.

$$T_{\text{eff}} = \frac{\int_0^t P_{\text{mpp}}}{\int_0^t P_{\text{pv}}} \cdot 100 \quad (5)$$

A. Under Standard Test Condition (STC)

It is discovered that the array output power at STC is 238.2 W. The current conditions include an ambient temperature of 25°C and radiation of 1000 W/m². Fig. 9(a) shows the power output comparison of the three MPPT methods at STC. Here, it is noted that tracking the MPP takes roughly 0.119 s for the P&O, 1.457 s for the PSO, and 0.646 s for the CS MPPT algorithms. P&O, PSO, and CS have tracking efficiency of 99.8%, 99.9%, and 99.8%, respectively. P&O's time reaction in this instance is superior to that of the other two techniques. The PSO approach requires the longest time to monitor MPP while maintaining tracking efficiency that is comparable to the other two methods.

B. Under Partial Shading Condition (PSC)

In this instance, the temperature was adjusted to 25°C, but the radiation on the four series-connected PV modules is varied, measuring 1000, 800, 400, and 600 W/m², respectively. The global maximum power point in this instance was determined to be 116.2 W. Fig. 9(b) compares the power output of the three MPPT techniques when there is partial shading. It was shown that the PSO and CS algorithms take 0.943 and 0.472 seconds, respectively, to track GMPP (i.e., 116.2 W). In contrast, at about 95.56 W, the P&O algorithm becomes stuck at a local maximum point. Under partial shading conditions, the tracking efficiencies of the PSO and CS MPPT algorithms are both 99.65%, however the P&O approach has a poor tracking efficiency of 82.23%. In this instance, PSO and CS have far higher accuracy than P&O algorithm.

C. Under Fast Varying Solar Radiation (FVSR)

The PV array receives the fast-changing radiation (Fig. 10(a)) as a step signal. Fig. 10 (b) shows the power output response of the three MPPT algorithms to this rapidly varying radiation. It is discovered that the P&O algorithm tracks the MPP with the fastest tracking efficiency (0.077s) from 0-1s of simulation (99.8%). Here, the PSO and CS follow the MPP with tracking efficiency of 99.8% and 99.9% in 0.55 s and 0.65 s, respectively. The P&O tracks the new MPP in 0.05 s with a tracking efficiency of 984.2% after a sudden change in solar irradiance (at 1 s). PSO and CS require 0.11 and 0.13 seconds, respectively, to track the MPP with tracking efficiency of 99.2 % and 99.774 %, respectively. In this case as well MPP tracking by CS has better accuracy and fast tracking.

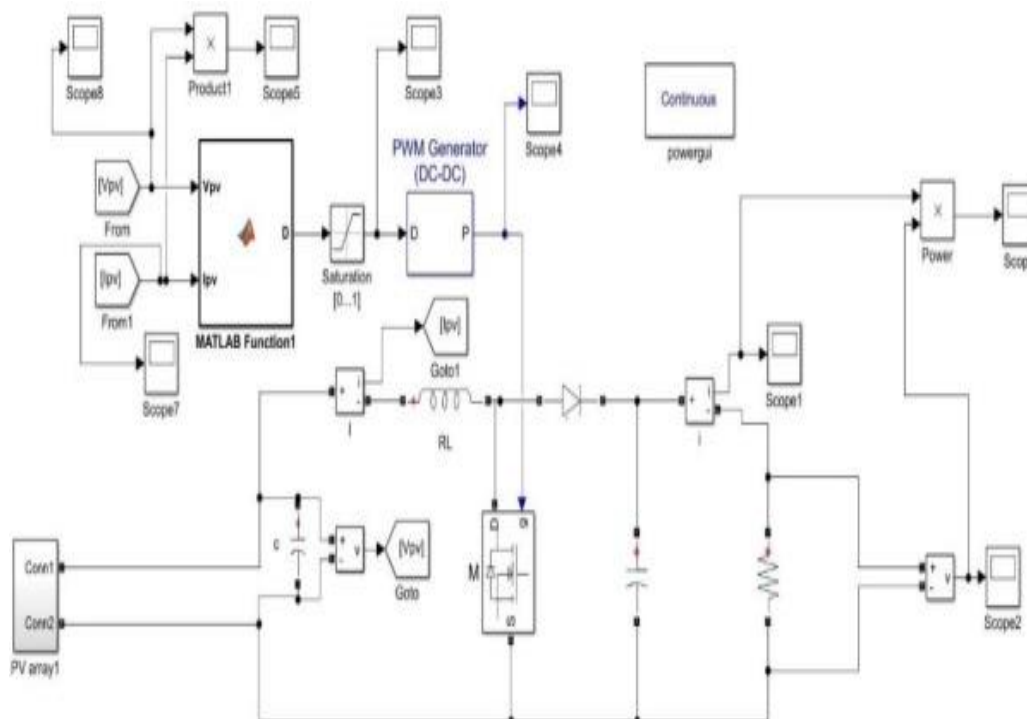
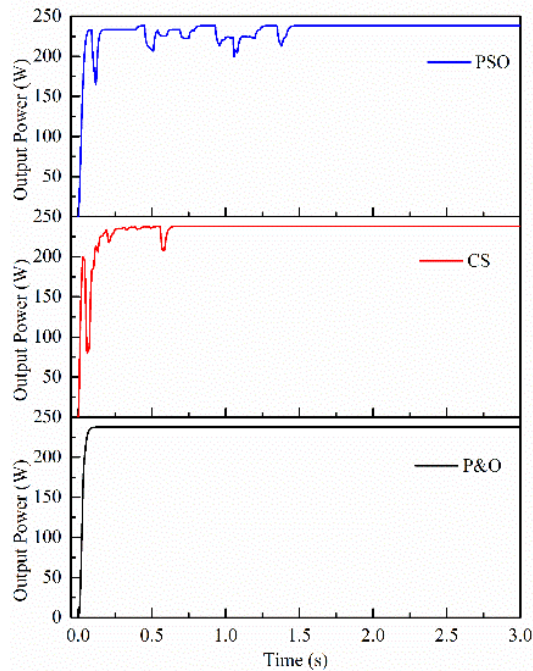
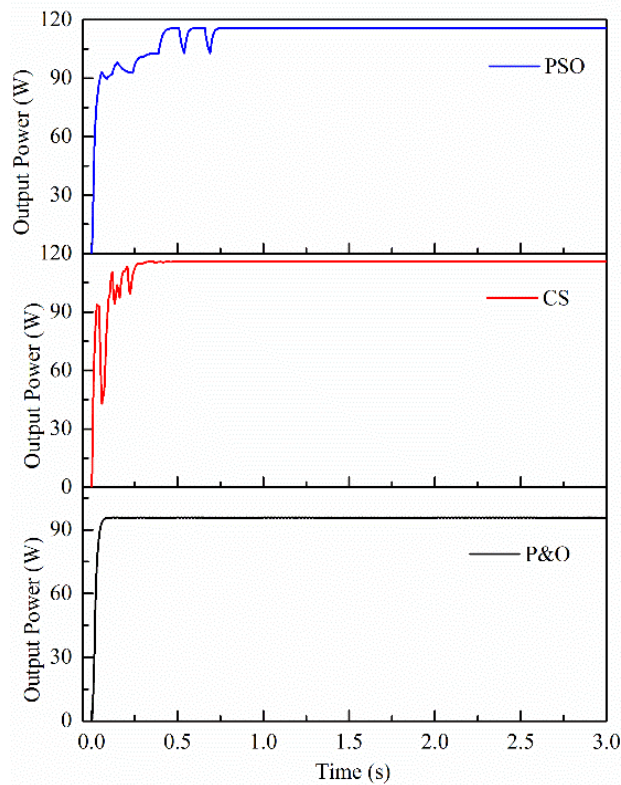


Fig. 8. Model of PV array with boost converter in Simulink

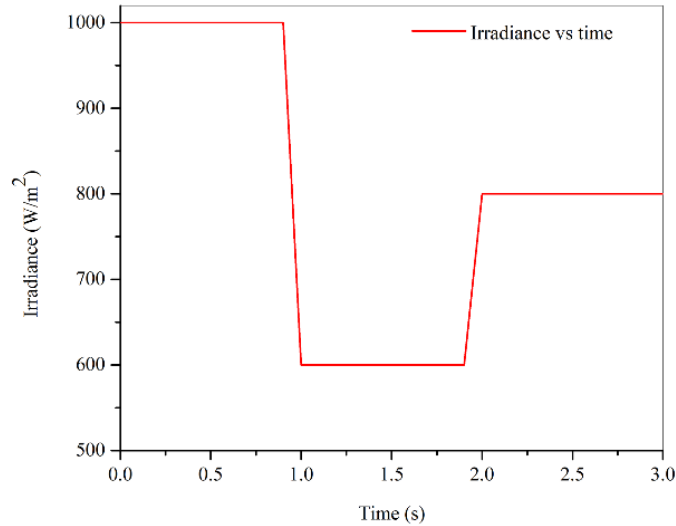


(a)

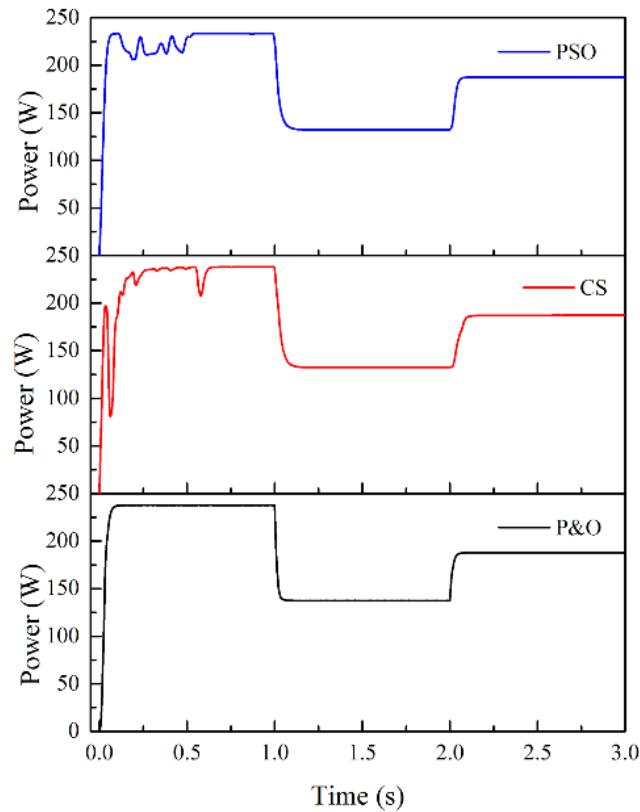


(b)

Fig. 9. Comparison of power output from PSO, CS and P&O (a) at STC (b) under PSC



(a)



(b)

Fig. 10. (a) Fast changing solar irradiance input, (b) Power output comparison of PSO, CS and P&O under FVSR

V. CONCLUSION

This study compares three MPPT algorithms (P&O, PSO, and CS) using a MATLAB Simulink model. The tracking accuracy, tracking time, and tracking efficiency of these MPPT techniques are contrasted. Three situations were used to compare the methods: STC, partial shade, and rapidly changing irradiance. The MPP was tracked under STC in 0.119 seconds with a 99.8% tracking efficiency using the P&O method. PSO and CS approaches have tracked MPP with 99.65% efficiency in partial shade conditions; hence, these methods are considered to be superior to P&O. Additionally, the CS technique tracks the MPP in this instance faster (0.472 s) than the PSO method (0.55 s). When the radiation changed quickly, the CS technique was able to follow MPP in 0.13 seconds with 99.74% tracking efficiency. According to the simulation results, MPP is tracked by the CS approach under all three scenarios with the highest tracking efficiency.

REFERENCES

- [1]. Verma D, Nema S, Shandilya AM, Dash SK. Maximum power point tracking (MPPT) techniques: Recapitulation in solar photovoltaic systems. *Renewable and Sustainable Energy Reviews*. 2016 Feb 1;54:1018-34.
- [2]. Salam Z, Ahmed J, Merugu BS. The application of soft computing methods for MPPT of PV system: A technological and status review. *Applied Energy*. 2013 Jul 1;107:135-48.
- [3]. Mohanty P, Bhuvaneshwari G, Balasubramanian R, Dhaliwal NK. MATLAB based modeling to study the performance of different MPPT techniques used for solar PV system under various operating conditions. *Renewable and Sustainable Energy Reviews*. 2014 Oct 1;38:581-93.
- [4]. Ahmed J, Salam Z. An improved perturb and observe (P&O) maximum power point tracking (MPPT) algorithm for higher efficiency. *Applied Energy*. 2015 Jul 15;150:97-108.
- [5]. Rezk H, Fathy A, Abdelaziz AY. A comparison of different global MPPT techniques based on meta-heuristic algorithms for photovoltaic system subjected to partial shading conditions. *Renewable and Sustainable Energy Reviews*. 2017 Jul 1;74:377-86.
- [6]. Mosaad MI, abed el-Raouf MO, Al-Ahmar MA, Banakher FA. Maximum Power Point Tracking of PV system Based Cuckoo Search Algorithm; review and comparison. *Energy Procedia*. 2019 Apr 1;162:117-26.
- [7]. Koad RB, Zobaa AF. Comparison between the conventional methods and PSO based MPPT algorithm for photovoltaic systems.
- [8]. Ahmed J, Salam Z. A soft computing MPPT for PV system based on Cuckoo Search algorithm. In 4th International Conference on Power Engineering, Energy and Electrical Drives 2013 May 13 (pp. 558-562). IEEE.
- [9]. Wang Y, Yang Y, Fang G, Zhang B, Wen H, Tang H, Fu L, Chen X. An advanced maximum power point tracking method for photovoltaic systems by using variable universe fuzzy logic control considering temperature variability. *Electronics*. 2018;7(12):355.
- [10]. Faranda R, Leva S. Energy comparison of MPPT techniques for PV Systems. *WSEAS transactions on power systems*. 2008 Jun 1;3(6):446-55.
- [11]. Go, S. I., Ahn, S. J., Choi, J. H., Jung, W. W., Yun, S. Y., & Song, I. K. Simulation and analysis of existing MPPT control methods in a PV generation system. *Journal of International Council on Electrical Engineering*. 2011;1(4), 446-451.
- [12]. Ishaque K, Salam Z, Amjad M, Mekhilef S. An improved particle swarm optimization (PSO)-based MPPT for PV with reduced steady-state oscillation. *IEEE transactions on Power Electronics*. 2012 Jan 23;27(8):3627-38.



- [13]. Ishaque K, Salam Z. A review of maximum power point tracking techniques of PV system for uniform insolation and partial shading condition. *Renewable and Sustainable Energy Reviews*. 2013 Mar 1;19:475-88.
- [14]. Yang XS, Deb S. Multiobjective cuckoo search for design optimization. *Computers & Operations Research*. 2013 Jun 1;40(6):1616-24.
- [15]. Nugraha DA, Lian KL. A Novel MPPT Method Based on Cuckoo Search Algorithm and Golden Section Search Algorithm for Partially Shaded PV System. *Canadian Journal of Electrical and Computer Engineering*. 2019 Jul 23;42(3):173-82.
- [16]. Mohapatra A, Nayak B, Das P, Mohanty KB. A review on MPPT techniques of PV system under partial shading condition. *Renewable and Sustainable Energy Reviews*. 2017 Dec 1;80:854-67.
- [17]. Belkaid A, Colak I, Isik O. Photovoltaic maximum power point tracking under fast varying of solar radiation. *Applied energy*. 2016 Oct 1;179:523-30.